Proceedings of the 8th International Conference on MicroManufacturing
University of Victoria, Victoria, BC, Canada, March 25-28, 2013

Prevention of Self-excited Vibrations in End-milling by Actively Tuning Fixture Stiffness using Fixed-fixed Beams Under Axial Load

ICOMM 2013 No. 111

Paul M. Moore[1], Gloria J. Wiens[2]
[1]Paul M. Moore; Mechanical & Aerospace Engr., University of Florida, USA; e-mail: paulmoor@ufl.edu
[2]Gloria J. Wiens; Mechanical & Aerospace Engr., University of Florida, USA; e-mail: gwiens@ufl.edu

ABSTRACT

In this paper, the development of a novel workpiece holder for micro- and meso-scale applications is discussed. Through the use of applied tensile axial force on fixed-fixed support beams, the stiffness and clamping force of the fixture can be actively tuned. Additionally, by applying varying stiffness values to two or more fixture elements working in tandem, the position of the workpiece can be manipulated. By tuning the stiffness, it was shown that the stable cutting region of end-milling operations can be effectively increased to allow for greater material removal. Other improvements in cutting operations can be achieved by using the part manipulation capability of the fixtures to make corrections in the position of the part during machining and by using the force tuning capability to reduce part deformation due to over-clamping.

INTRODUCTION

One of the most common problems that occur during milling is the self-excited vibration of cutting tools, also known as chatter, which adversely affects surface finish, dimensional accuracy, tool life and machine life. Self-excited vibrations are caused by instability in the cutting process that occurs when the cutting profile of a tooth is in phase with that of a previous tooth. This produces a forced vibration that can become unstable if it matches the harmonic frequency of the cutting tool [1].

The study of self-excited vibration has a long history, which can be traced back to Tlusty, Merritt and Tobias [1-3], who developed an approach for predicting self-excited vibrations called the stability lobe approach. The end result of the approach is typically a diagram that shows the regions of stable and unstable machining operations in terms of depth of cut with respect to spindle speed. Fig. 1 shows the plots of stability lobes for two machine stiffness cases (k_1 and k_2). For each stiffness case, a stable operation condition exists for all set of values (spindle speed, depth of cut) that lie below the stability lobe curve. The diagram can be used to find the critical axial depth of cut, the threshold for which stable cutting can be achieved at all spindle speeds; the chatter frequencies of the machining operation, where maximum machine chatter is observed; and the spindle speeds that provide the maximum stable axial depth of cuts.

When the stiffness and natural frequency of a cutting tool are modified, the stability lobes of a given machining operation shift. When the stiffness is increased, the lobes shift upward and when the natural frequency is increased, the lobes shift to the right in the stability lobe diagram [4]. Since the natural frequency of a cutting tool is dependent upon its stiffness, the result is that an increase in tool stiffness shifts the lobes toward larger depth of cuts and higher frequencies. This relationship has led to the development of larger and heavier cutting tools and fixtures, which have greater stiffness but are also more expensive and take up more space. Additionally, achieving higher stiffness through excessive clamping force can result in part deformation or non-uniform cutting force. For these reasons, the optimization of the cutting tool stiffness [5, 6] and clamping force [7] has received much attention.

The actively tuned fixturing device being discussed in this paper, shown in Fig. 2, was designed specifically for micro- and meso-scale machining applications due to the unique challenges associated with fixturing at the micro- and meso-scale and the characteristics of the miniaturized machine tools (mMTs) used in these applications. These applications are also well suited for such a device due to the small amount of tensile force needed to achieve the stiffness require for fixturing.

When a miniaturized machine tool is developed, its dynamic characteristics are one of the key considerations taken into account. Of all the dynamic properties of the mMT, rigidity is of the utmost concern since it generally affects machining errors of the part under the action of various forces. For many decades, machinists have depended upon the circular tool path assumption to make accurate predictions in machining dynamics. This theory has been used to very accurately predict machining characteristics such as cutting

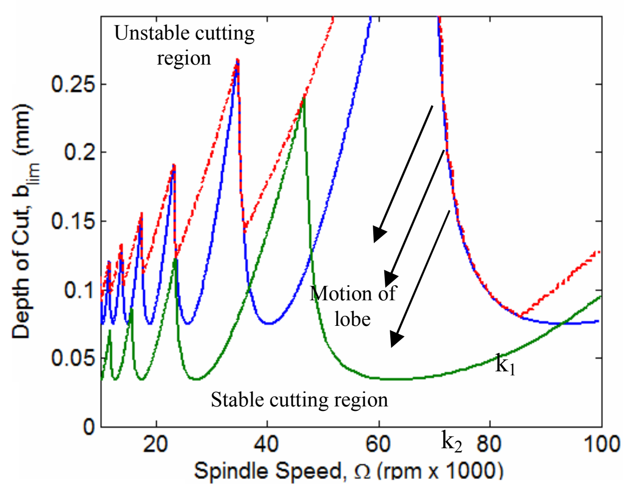

Fig. 1: Stability lobe plot showing the path of the lobes as fixture stiffness is decreased, where the dotted line shows the effective stable region with stiffness tuning

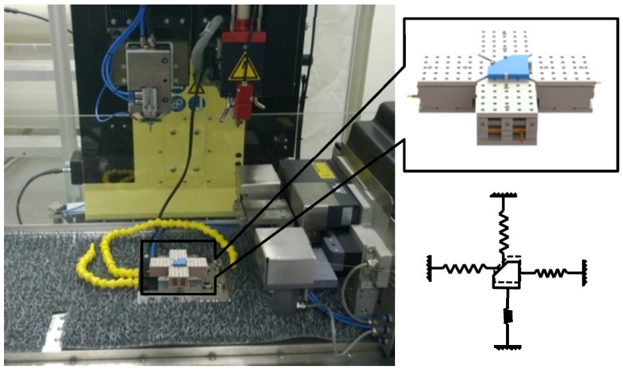

Fig. 2: Two-DOF configuration of fixturing device consisting of four Adaptively Tuned microManipulators

forces, maximum depths of cut and chatter frequencies in the macroscale but has been found to be less suitable in the microscale. This departure from the norm is due to the much higher spindle speeds used in micro-scale endmilling, which result in higher feed per tooth to tool radius ratios (f_t/r) and thus non-circular paths. Other large discrepancies appear due to the increased ratio of runout to tool radius (r_o/r), which changes the cutting force characteristics [8,9]. Additionally, since many micro-endmills use two-flute cutting tools, an increase in tool runout will cause one of the cutting edges to perform almost all of the cutting. The runout may result in rapid tool wear and cause the system to become unstable at certain spindle speeds, leading to self-excited vibration at half the expected chatter frequency.

By developing a fixturing device capable of actively tuning its stiffness, optimal machining dynamics can be achieved for a wide range of end-milling operations. This ability can lead to a much larger effective stable cutting range, as can be seen in Fig. 1. In the figure, a plot of two stability lobes for a typical micro-milling operation is given. The dotted line traces the path of the peaks of the lobes, which shows the effective stable cutting region for the whole range of stiffness values. One such fixture would use the deflection of fixed-fixed beams to provide a desired stiffness. It was also demonstrated that by selectively tuning the stiffness of the fixture, a reduction in machining error due to tool runout was achievable [10]. In this paper, subjecting these beams to axial loads is explored as an alternative approach to actively tuning the stiffness.

DEVELOPMENT OF FIXTURE

A. END-MILL STIFFNESS CHAIN

Since the components of end-mills are typically arranged in series with one another, the overall stiffness of end-mills is highly dependent upon the least stiff component. In most cases, this component is the cutting tool itself, which can be approximated as a cantilever beam subjected to a transverse load at its free end [6]. As such, the stiffness of an end-mill can be described by the following equations:

$$K_E = \left(\frac{1}{K_T} + \frac{1}{K_F} + \frac{1}{K_S}\right)^{-1} \quad (1)$$

$$K_T = \frac{3E_T I_T}{L_T^3} \quad (2)$$

where K_E is the effective stiffness of the end-mill, K_T is the stiffness of the cutting tool, K_F is the stiffness of the fixture, K_S is the stiffness of the remaining end-mill structure, E_T is the Young's modulus of the tool, I_T is the area moment of inertia of the tool and L_T is the length of the tool.

Due to the fact that the components are arranged in series, in order to tune the overall stiffness, the fixture stiffness should be approximately equal to that of the cutting tool given in (1). This will allow for the capability to make significant changes in the effective stiffness of the end-mill without compromising the overall stiffness. In this paper, the fixture is being developed so that it is capable of achieving stiffness equal to that of a carbide cutting tool with a length of 8 mm and a diameter of 1 mm, which is assumed to be the largest tool that would be used in a meso-scale machining operation. Smaller tools tend to have lower stiffness so it is assumed that any other tools used in meso-scale or micro-scale machining will be less stiff. By solving (2), the tool stiffness was found to be 57.52 kN/m.

B. STIFFNESS OF FIXED-FIXED BEAMS UNDER AXIAL LOAD

In order to determine the necessary size and material properties of the fixed-fixed beams, the mechanical and vibrational properties of the beam must be understood. The governing differential equation for the transverse displacement, $y(x,t)$, of a fixed-fixed beam under axial tension load at distance (x) is given by the following equation as a function of time, (t) [11]:

$$\frac{\partial^2}{\partial x^2}\left[EI(x)\frac{\partial^2}{\partial x^2}y(x,t)\right] - P\frac{\partial^2 y(x,t)}{\partial x^2} - \rho A\omega^2 y(x,t) = 0 \quad (3)$$

where E is the Young's modulus, $I(x)$ is second moment of area along the beam, $y(x,t)$ is the transverse deflection of the beam, P is the axial tensile load, ρ is the mass density of the beam material the length, A is the cross-sectional area, and ω is the circular natural frequency. The solution of the differential equation can be written as:

$$Y(x) = c_1 sinhM\zeta + c_2 coshM\zeta + c_3 sinN\zeta + c_4 cosN\zeta \quad (4)$$

where $c_1, c_2, c_3, c_4, c_1, M$, and N are unknown constants and ζ is the normalized x. This function gives us the vibrational modes shapes of the beam.

$$\zeta = \frac{x}{L} \quad (5)$$

Since the beam is clamped on both ends, the following boundary conditions may be applied:

$$Y(x)|_{x=0} = 0, \quad Y(x)|_{x=L} = 0,$$
$$\left.\frac{dY(x)}{dx}\right|_{x=0} = 0, \quad \left.\frac{dY(x)}{dx}\right|_{x=L} = 0 \quad (6)$$

By substituting the boundary conditions into (4) and letting $c_1 = 0$, the coefficients can be given as the following.

$$c_1 = 1, \quad c_2 = \frac{MsinN - NsinhM}{N(coshM - cosN)}$$
$$c_3 = -\frac{M}{N}, \quad c_4 = -\frac{MsinN - NsinhM}{N(coshM - cosN)} \quad (7)$$

Additionally, from [12], the variables $M$and N are given as:

$$M = L\left\{\frac{P}{2EI} + \left[\left(\frac{P}{2EI}\right)^2 + \left(\frac{\rho A}{EI}\right)\omega^2\right]^{1/2}\right\}^{1/2}$$

$$N = L\left\{-\frac{P}{2EI} + \left[\left(\frac{P}{2EI}\right)^2 + \left(\frac{\rho A}{EI}\right)\omega^2\right]^{1/2}\right\}^{1/2} \quad (8)$$

Finally, by substituting (7) and (8) into the solution (4) and applying the boundary conditions (6) the natural frequency can be found. In order to accomplish this task, the roots of $Y(x = 0, \omega^2) = 0$ were found, where the value of ω^2 at the first root gives us the natural frequency of the first mode and so on for further roots and modes.

Given that the beams are to be made of spring steel with a length of 36 mm and width of 5 mm and thickness of 0.375 mm, the effects of axial tension load can be found. In Fig. 3, the natural frequency found by solving is plotted with respect to the tensile load.

In order to find the stiffness of the beam with respect to the axial load, the modal mass must first be found. Solving when the tension is zero, the modal mass for the first mode is given by:

$$k_{P=0} = \frac{192EI}{L^3} \quad (9)$$

$$m_{n=1} = \left.\frac{k}{\omega_{n=1}^2}\right|_{P=0} \quad (10)$$

where $m_{n=1}$ is the modal mass of the first mode and $\omega_{n=1}^2$ is the natural frequency from Fig. 3 when the axial tensile load is zero. Finally, the stiffness of the fixture with respect to axial tensile load can be found assuming that the modal mass is constant with respect to the load. Since the fixture consists of two fixed-fixed beams in parallel, the stiffness of the fixture is equal to the sum of the stiffness of the two beams. These assumptions yield the following equation for fixture stiffness.

$$K_F(P) = 2m_{n=1}\omega(P)_{n=1}^2 \quad (11)$$

A plot of the fixture stiffness with respect to axial tensile load is given in Fig. 4. In this figure, it can be shown that fixture stiffness is equal to the tool stiffness when the axial tensile load in each beam is 43 N. It can also be shown that the amplification of stiffness as a result of a 50 N load as opposed to no load is about 1.69.

C. FIXTURE DESIGN

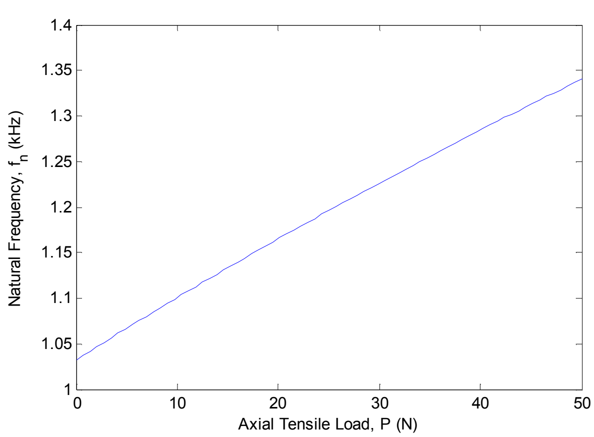

Fig. 3: Natural frequency of fixed-fixed beam with respect to the beam's tensile load

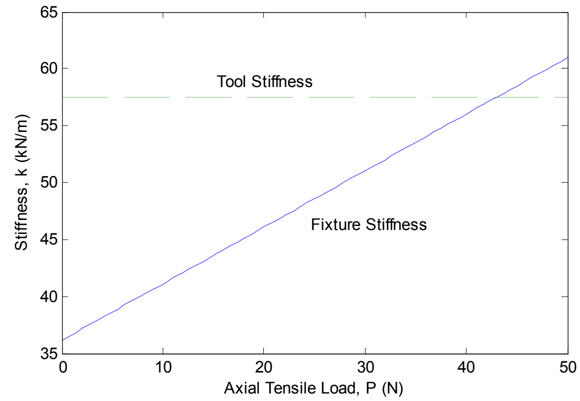

Fig. 4: Fixture stiffness for two fixed-fixed beams with respect to axial tension, which is equal to the tool stiffness when the tension in each beam is equal to 43 N

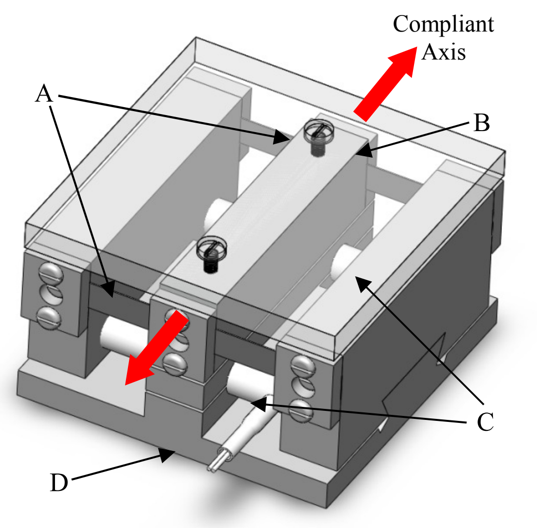

Fig. 5: Design of apparatus showing (A) fixed-fixed beams, (B) center bar, (C) piezo actuators, (D) ground plate, where the large arrows show the compliant axis

The preliminary design of the fixture, shown in Fig. 5, is based on previous work related to compliant fixturing [13, 14]. It is composed of two fixed-fixed beams attached to a center bar that supports a platform upon which workpieces may be fixed. The beams are placed under axial tension load by two piezo actuators. This arrangement allows for stiffness tuning in one direction but can be combined with a similar unit rotated 90° along the z-axis in order to achieve complete stiffness tuning in the plane. The device utilizes two large-load piezo-actuators to apply tension to the beams. The beams are attached to a bar halfway down the length of each beam. The bar can move freely along the transverse axis of the beam. Since the bar prevents rotation at the point along the length of the beam where $x = (1/2)L$, all even-numbered modes are eliminated. As can be seen in Fig. 6, every even mode has a non-zero slope at this point while all odd modes have a slope of zero. However, we are most interested in the first mode since it is used to determine the stability of the machining process and will be the mode must affected by the machining process because it has the lowest frequency.

PART MANIPULATION USING MULTIPLE FIXTURES

In order to demonstrate how the tuning of stiffness and contact force is achieved, a one-DOF configuration of the mechanism is shown in Fig. 7. In this configuration, the part can be moved side-to-side by altering the stiffness of the two fixturing devices. By pre-loading the fixtures with an appropriate amount of compression, the part can maintain equal contact forces on each side. Additionally, by modifying the spring stiffness of the two fixture elements independently, a change in the equilibrium position of the part can be achieved. For example, if the left spring is made stiffer while the right spring is made less stiff, the contact forces may remain the same while the part shifts toward the softer spring to find its equilibrium. Alternatively, the position of the part can be maintained while the contact force is modified by changing the stiffness of both springs simultaneously. Fig. 8 demonstrates this capability by representing each fixture element as a preloaded spring.

In order to determine the effectiveness of this compliant fixturing approach in terms of workpiece manipulating capabilities, the displacement of the workpiece with respect to the beam stiffness is found. By assuming that the spring forces of the two fixturing elements are equal and constant, and that the springs begin with equal stiffness values, the following equation can be found:

$$\Delta y = \frac{F_P}{k_P+\Delta k} - \frac{F_P}{k_P} \quad (12)$$

where Δy is the displacement of the workpiece, F_P is the axial preloaded tensile force in the beams, k_P is the preloaded stiffness of the beams, and Δk is the change in stiffness of the beams. The results of this function were plotted for the entire range of stiffness and preloaded force values and are shown in Figs. 8 and 9. Since the stiffness values are not independent of one another, the plots show just one of the beam stiffness values. It was shown that for the various preloaded stiffness, the range of motion does not change but is shifted toward the dependent beam as the independent preloaded beam stiffness increases. In Fig. 10, the preloaded axial tensile force was modified, showing that the larger preloaded forces resulted in larger ranges of displacement. In fact, the range of displacement is exactly proportional to the preloaded force, as can be gathered from (12).

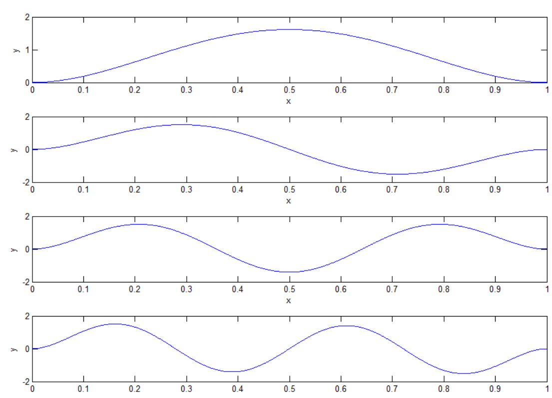

Fig. 6: First four mode shapes of a fixed-fixed beam, showing that the even-numbered modes must be eliminated due to their non-zero slops at $x = (1/2)L$

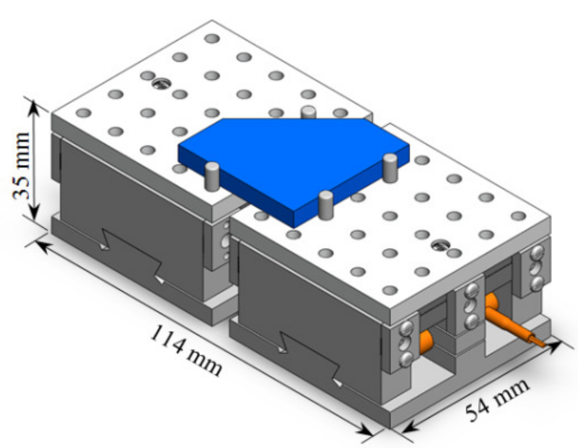

Fig. 7: One-DOF fixturing configuration capable of stiffness tuning and part manipulation

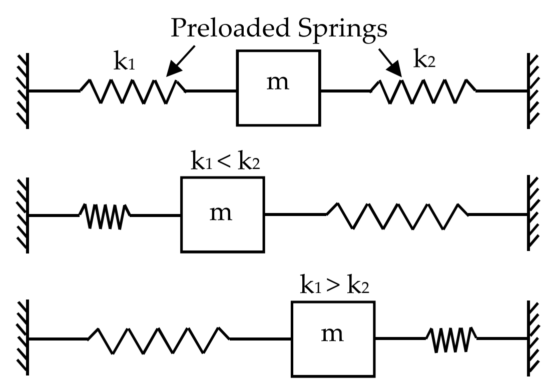

Fig. 8: (Left) One-DOF fixture configuration holding a part and (right) lumped-mass model showing how altering the stiffness of pre-loaded springs can be used to manipulate a part

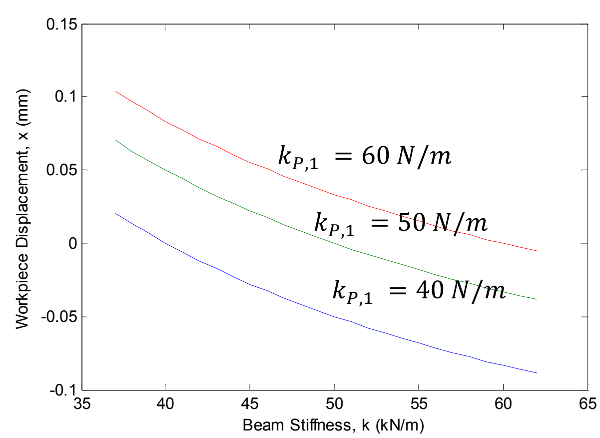

Fig. 9: Workpiece displacement with respect to beam stiffness of one of the fixture elements, shown for varying preloaded axial tensile stiffness values

The configuration of fixtures discussed above allows for stiffness tuning and workpiece manipulation along one axis. This capability can be very useful if proper care is taken to align it with the direction of the end-mill cutting force. However, having two degrees of freedom for stiffness tuning and manipulation could yield much better results. For example, it might be advantageous to have a much stiffer axis in the cutting tool's radial direction than in its tangential direction or vice versa. In order to achieve this level of control a minimum of three fixture elements must be used but in order to reduce the coupling effects between the fixture elements, it would be more advantageous to use four. Even so, the coupling effect between the axes is of great concern. In Fig. 11, a two-DOF fixture configuration is depicted. In the figure, four pins are used to hold an arbitrary workpiece. Since the workpiece is assumed to be much stiffer along the axis of the beams than in the transverse direction, motion of the pin is restricted to the transverse direction. Since the workpiece shown in the figure has contact surfaces that are not normal to the beams' transverse directions associated with the pins, these pins will slide with respect to the workpiece surface. Fig. 12 shows a part being manipulated, where the contact surface for the pins varies depending on the geometry. In the figure, the two springs along the vertical axis, $k_{y,1}$ and $k_{y,2}$, are being modified in order to move the part downward. As a result, the left spring, $k_{x,1}$, is elongated while the right spring, $k_{x,2}$, does not change in length. The contact points for both the left and right spring move along the surface of the workpiece. This relationship will vary for every workpiece shape so a control system will need to be developed in order to characterize the coupling between the fixtures before machining can occur.

SUMMARY OF RESULTS

It was shown that axial tension in fixed-fixed beams can, in theory, be used for tuning fixture stiffness and clamping force. By characterizing the vibrational characteristics of the beam with respect to the axial tension it was shown that the values of stiffness and natural frequency of the fixture can closely match those needed to improve the machining stability. Furthermore, the range of stiffness capable with axial tension applied by currently available piezo-actuators proved to be sufficiently large to allow for manipulation of the part up to 0.35 mm, which is adequate in the micro- and meso-scale domain for end-milling assembly and other common tasks. The greatest range of manipulation was associated with systems that started with large preloaded axial tension forces while those that started with large stiffness values on one beam and small stiffness values on another had approximately the same range of motion as configurations with equal stiffness values for both fixtures.

By assuming that the end-mill structure stiffness, K_S, from (1) is significantly larger than the tool and fixture stiffness and can therefore be omitted, the range of the effective stiffness, K_E, was found. This range was used to create a new stability lobe diagram for the two-DOF system shown in Fig. 11. By integrating under the curves for the original stability lobe and the effective stability lobe, shown in Fig. 13, it was found that a 7% increase in the stable cutting region can be achieved with this first conceptual fixture design. While this improvement is extremely modest, it proves the concept that reductions in self-excited vibrations can be achieved.

CONCLUSION AND FUTURE WORK

The work presented in this paper represents a small step

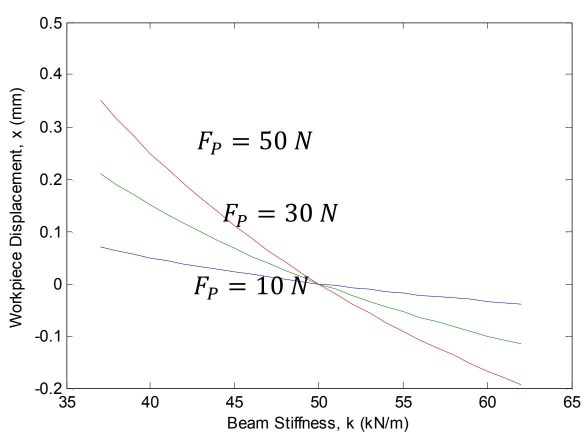

Fig. 10: Workpiece displacement with respect to beam stiffness for varying preloaded axial tensile force values

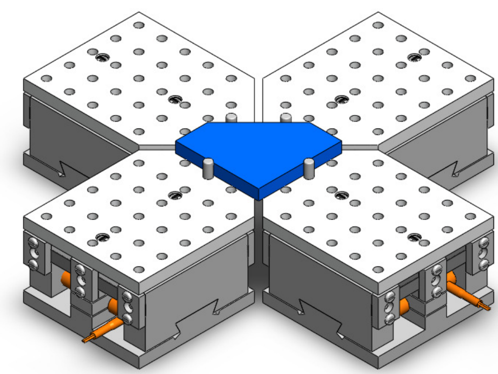

Fig. 11: Two-DOF configuration of the fixturing apparatus using four fixture elements

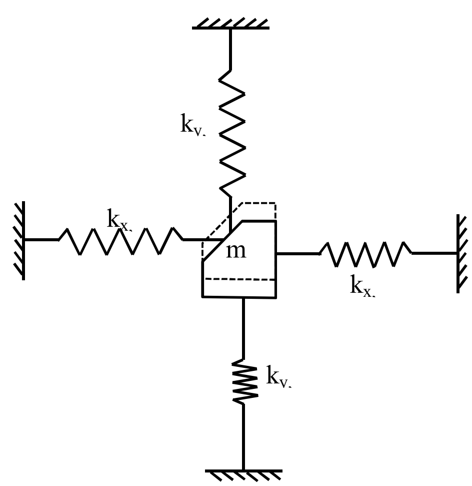

Fig. 12: Lumped parameter model of the two-DOF fixturing apparatus

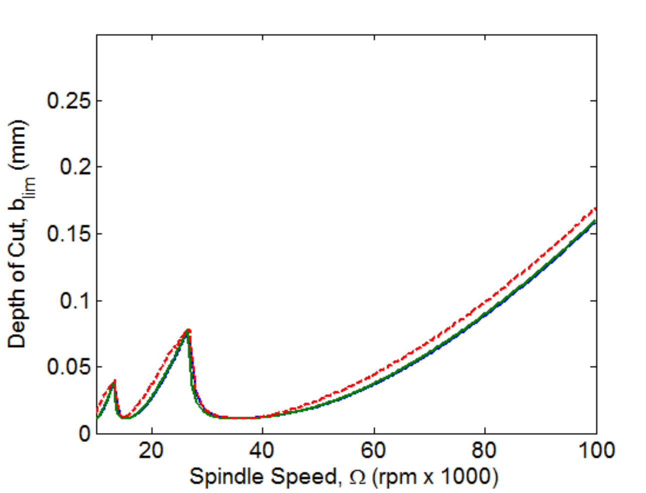

Fig. 13: Stability lobe diagram for fixture and tool in series with the improved stable cutting region.

toward the goal of actively tuning the machining dynamics during micro- and meso-scale machining in order to improve manufacturing quality and performance in this very exciting field. While a 7% improvement in stability for end-milling may not be a game-changer for micro- and meso-scale manufacturing, it is likely that some optimization techniques can be performed to increase this gain. Furthermore, this research was carried out using a very conservative estimate for tool stiffness. If one were to carry out the same analysis for a smaller tool, or solved the stiffness using the second area of moment of the actual tool rather than a circular approximation, the performance gains would be greater.

The future work related to this research first involves optimizing the beam dimensions now that their relationship with end-milling stability is understood. Secondly, the coupling relationship between the fixtures in the two-DOF configuration will be analyzed. Next, prototype fixtures will be designed in order to experimentally validate the theory presented in this paper. Based on the experimental result, the fixture design will be finalized and sensors will be integrated along with a built-in control system. This will allow the fixture to close the loop with the machine in terms of position and force. Since the tension is being applied by piezo-actuators, it is possible to control these variables with very little latency.

ACKNOWLEDGEMENTS

This study was supported by the University of Florida Department of Mechanical and Aerospace Engineering Alumni Fellowship.

REFERENCES

[1] J. Tlusty, W. Zuton, F. Ismail, "Stability Lobes in Milling," *Annals of the CIRP*, 1983; 32(1): pp. 1-5.

[2] H.E. Merritt, "Theory of Self-Excited Machine-Tool Chatter," *J. of Eng. for Industry*, 1965; 87(4): pp. 447-454.

[3] S.A. Tobias, "Vibration of Machine Tools," *The Production Engineer*, 1964; 43(12): pp. 559-608.

[4] P.M. Moore, G.J. Wiens, T.B. Rippere, "Active Compliant Interface Mechanism (ACIM) for Dynamic Tuning of Meso-scale Machine Tools," *ICOMM:* 2011, No. 17.

[5] K.S. Kumar and G. Paulraj, "Analysis and optimization of fixture under dynamic machining condition with chip removal effect," *J. of Intelligent Mfg.*, 2012; pp. 1-14.

[6] M.A. Salgado, L.N. López de Lacalle, A. Lamikiz, J. Muñoa, J.A. Sánchez, "Evaluation of the stiffness chain on the deflection of end-mills under cutting forces," *Int. J. of Mach. Tools and Man.*, 2005; 45(6): pp. 727-739.

[7] S.G. Chen, A.G. Ulsoy, Y. Koren, "Computational Stability Analysis of Chatter in Turning," *ASME J. of Mfg. Sci. and Eng.*, 1997; 119(40): pp. 457-460.

[8] W.Y. Bao, and I.N. Tansel, "Modeling micro-end-milling operations. Part I: analytical cutting force model," Int. Journal of Mach. Tools & Manu., 2000; 40: pp. 2155-2173.

[9] W.Y. Bao, and I.N. Tansel, "Modeling micro-end-milling operations. Part II: tool run-out." Int. Journal of Mach. Tools & Manu., 2000; 40: pp. 2175-2192.

[10] T.B. Rippere, K.J. Rao, G.J. Wiens, "Modeling and Analysis of Fixel Design for Micromanufacturing Active Fixturing," *J. of Mfg. Sci. and Eng.*, 2011; 133: pp. 1-4.

[11] L. Meirovitch, Analytical Methods in Vibration, Macmillan, New York: 1967, pp. 464-453.

[12] A. Bokaian, "Natural Frequencies of Beams Under Tensile Axial Loads," *J. of Sound and Vib.*, 1990, 142(3): pp. 481-498.

[13] P.M. Moore, M. Rakotondrabe, C. Clevy, "Development of a Modular Compliant Microassembly Platfom with Integrated Force Measurement Capabilities," *ICOMM*: 2012, No. 93.

[14] M. Rakotondrabe et al., "Presentation, Force Estimation and Control of an Instrumented Platform dedicated to Automated Micromanipulation Tasks," *IEEE Conf. on Auto. Sci. and Engr.*: 2010, pp. 722-727.